

# Leiomyosarcoma of the Inferior Vena Cava - An Experience from a Tertiary Care Centre in South India

Aleena Elizabeth Andrews<sup>1</sup>, Juvaina Puthiyakam<sup>2</sup>, Naufal Perumpalath<sup>3</sup>, Devarajan Ellezhuthil<sup>4</sup>

<sup>1</sup>Department of Radio Diagnosis, Government Medical College, Thrissur, Kerala, India.

<sup>2, 3, 4</sup> Department of Radio Diagnosis, Government Medical College, Kozhikode, Kerala, India.

## ABSTRACT

### BACKGROUND

Leiomyosarcomas (LMS) of inferior vena cava (IVC) are rare smooth muscle sarcomas with less than 300 cases described in the literature. Leiomyosarcoma of IVC is, often detected late in the course due to its indolent manifestation. This study intends to discuss the experiences and challenges in diagnosing this rare entity primarily by radiological imaging in a tertiary centre in India.

### METHODS

This is a retrospective analysis of computed tomography (CT) and ultrasound findings in 6 cases of leiomyosarcoma of inferior vena cava who were referred for multidetector computer tomography (MDCT) scan in the Department of Radiodiagnosis of Government Medical College Calicut over the past 7 years by the treating physician. The patients were identified using a prospectively maintained database.

### RESULTS

In this study, there were six patients diagnosed as leiomyosarcoma of IVC, age ranging from 35 and 64 years (mean 47.8 years, SD 10.7) with 4 (66.6 %) females and 2 (33.33 %) males. The mean size of the tumour at the time of diagnosis was 8.4 cm. The segment of IVC most commonly involved was middle segment in 5 patients (83.3 %). In this series, only a single case had tumour entirely confined within the lumen of inferior vena cava without extraluminal extension. Two out of six cases (16.66 %) had lung metastasis at the time of diagnosis. Two cases without metastasis or significant infiltration to adjacent organs were amenable to resection.

### CONCLUSIONS

Leiomyosarcoma of IVC is a rare tumour, often detected late in the course due to its indolent manifestation. High index of suspicion may help in the early diagnosis of so that early treatment can begin and improve the clinical outcome.

### KEYWORDS

Leiomyosarcoma, Inferior Vena Cava, Mesenchymal Neoplasms

*Corresponding Author:*

*Dr. Aleena Elizabeth Andrews,  
Mekkattukunnel House,  
Chakkoth Lane, Poonkunnam,  
Thrissur - 680002, Kerala, India.  
E-mail: aleenaelizabeth26@gmail.com*

*DOI: 10.18410/jebmh/2021/380*

*How to Cite This Article:*

*Andrews AE, Puthiyakam J, Perumpalath N, et al. Leiomyosarcoma of the inferior vena cava - an experience from a tertiary care centre in south India. J Evid Based Med Healthc 2021;8(24):2023-2028. DOI: 10.18410/jebmh/2021/380*

*Submission 19-02-2021,*

*Peer Review 26-02-2021,*

*Acceptance 26-04-2021,*

*Published 14-06-2021.*

*Copyright © 2021 Aleena Elizabeth Andrews et al. This is an open access article distributed under Creative Commons Attribution License [Attribution 4.0 International (CC BY 4.0)]*

## BACKGROUND

Leiomyosarcomas are mesenchymal neoplasms of smooth muscle cell origin.<sup>1</sup> Retroperitoneum is a common location for sarcomas, attributing to about 12 – 69 % of cases.<sup>2</sup> Primary vascular LMS is a rare entity of which, inferior vena cava (IVC) is the most common site.<sup>3</sup> Leiomyosarcoma of the inferior vena cava, described in fewer than 300 patients in the literature, is a rare clinical scenario.<sup>4</sup> It is a slow growing tumour, with indolent clinical manifestation. They are identified incidentally, once they are large enough to cause mass effect on adjacent structures.<sup>5</sup> However, imaging done for non-specific complaints, is probably the only way to catch these lesions at its inception, offering best possible surgical cure preserving adjacent vital organs.

This study intends to discuss the experiences and challenges in diagnosing this rare entity primarily by radiological imaging.

## METHODS

A retrospective chart review of patients who underwent multidetector computer tomography scan in the Department of Radiodiagnosis of Government Medical College Calicut over the past 7 years between January 2013 to December 2020, referred by treating physician was performed in this descriptive case series. The patients diagnosed with leiomyosarcoma of IVC were identified using a prospectively maintained database.

MDCT was performed (16 row, slice thickness 5 mm, rotation time 0.5 s, collimation 16 × 1.25 mm, pitch 1.75 : 1, interval 2.5 mm) before and after administration of intravenous iodinated contrast medium with enhanced scans acquired at 30 and 70 s (50 ml contrast medium bolus, flow rate of 3 ml/s) was performed.

Ultrasound images provided in some cases, were obtained prior to acquisition of CT, using 3.5 Hz curvilinear probe.

## RESULTS

A total of 75,562 patients underwent contrast enhanced computed tomography of abdomen from January 2013 to December 2020. Excluding cases of CT performed for abdominal trauma, known case of gastrointestinal/hepatic/pelvic malignancy there were 59,962 cases who were evaluated for non-specific complaints. Using prospectively maintained data base, only 6 cases were diagnosed as leiomyosarcoma of IVC.

The mean age of patients diagnosed as leiomyosarcoma of IVC was 47.8 years (SD 10.7) ranging from 35 and 64 years. There were 4 (66.6 %) females and 2 (33.33 %) males. The mean size of the tumour at the time of diagnosis was 8.4 cm. The most common presentation was non-specific abdominal pain.

Physical examination revealed lower limb oedema in 4 subjects (66.6 %). Palpable mass on physical examination

was detected in 2 out of 6 cases. The segment of IVC most commonly involved was middle segment in 5 patients (83.3 %). In this series, only a single case had tumour entirely confined within the lumen of inferior vena cava without extraluminal extension. Two out of six cases (16.66 %) had lung metastasis at the time of diagnosis. Two cases without metastasis or significant infiltration to adjacent organs were amenable to resection.

A summary of the demographic data, clinical presentation, and treatment of all the participants is given in Table 1.



**Figure 1.** A 48-year-old female with complaints of right sided abdominal pain and a large mass palpable in the right lumbar and epigastric region: coronal contrast enhanced computed tomography of abdomen shows the intraluminal component of lesion (black arrows) distending the middle segment of IVC with the ill-defined extraluminal component (yellow arrow) of the lesion abutting the abdominal aorta



**Figure 2a.** A 38-year-old female complaining of abdominal pain of 2 months duration (a): ultrasound with colour doppler showing a well-defined hypoechoic lesion in the right anterior pararenal space with intraluminal extension into infrahepatic inferior vena cava



**Figure 2b.** A 38-year-old female complaining of abdominal pain of 2 months duration (b): axial contrast enhanced computed tomography of abdomen showing heterogeneously enhancing lesion (black arrow) at the right suprarenal location closely abutting the IVC



**Figure 3.** A 55-year-old male complaining of right sided abdominal pain, vague abdominal mass, and bilateral pedal oedema, for a duration of one month: coronal contrast enhanced computed tomography of abdomen shows the heterogeneously enhancing lesion (black arrow) involving the suprarenal IVC (white arrow)

| Parameter                                  | Case 1                                                                                                                                                                                                                                                 | Case 2                                                                                                                                                                                                   | Case 3                                                                                                                                                                                                                 | Case 4                                                                                                                                                                                                                                                          | Case 5                                                                                                                                                                | Case 6                                                                                                                                                                                      |
|--------------------------------------------|--------------------------------------------------------------------------------------------------------------------------------------------------------------------------------------------------------------------------------------------------------|----------------------------------------------------------------------------------------------------------------------------------------------------------------------------------------------------------|------------------------------------------------------------------------------------------------------------------------------------------------------------------------------------------------------------------------|-----------------------------------------------------------------------------------------------------------------------------------------------------------------------------------------------------------------------------------------------------------------|-----------------------------------------------------------------------------------------------------------------------------------------------------------------------|---------------------------------------------------------------------------------------------------------------------------------------------------------------------------------------------|
| Age                                        | 48                                                                                                                                                                                                                                                     | 38                                                                                                                                                                                                       | 55                                                                                                                                                                                                                     | 47                                                                                                                                                                                                                                                              | 35                                                                                                                                                                    | 64                                                                                                                                                                                          |
| Sex                                        | F                                                                                                                                                                                                                                                      | F                                                                                                                                                                                                        | M                                                                                                                                                                                                                      | M                                                                                                                                                                                                                                                               | F                                                                                                                                                                     | F                                                                                                                                                                                           |
| Symptoms                                   | Abdominal pain                                                                                                                                                                                                                                         | Abdominal pain                                                                                                                                                                                           | Right sided abdominal pain                                                                                                                                                                                             | lower abdominal pain                                                                                                                                                                                                                                            | Back pain                                                                                                                                                             | Right sided abdominal pain and bilateral pedal oedema                                                                                                                                       |
| Physical examination                       | Large mass palpable in the right lumbar, epigastric and umbilical region.                                                                                                                                                                              | Nil                                                                                                                                                                                                      | vague mass in the right hypochondrium and bilateral pedal oedema                                                                                                                                                       | Bilateral lower limb oedema                                                                                                                                                                                                                                     | Oedema of bilateral lower limbs                                                                                                                                       | Bilateral pedal oedema                                                                                                                                                                      |
| Duration                                   | One month                                                                                                                                                                                                                                              | Two months                                                                                                                                                                                               | One month                                                                                                                                                                                                              | One month                                                                                                                                                                                                                                                       | One month                                                                                                                                                             | Two months                                                                                                                                                                                  |
| Ultrasound                                 | Mass extending to retroperitoneum and intraluminal into hepatic IVC.                                                                                                                                                                                   | well defined hetero echoic lesion in the right anterior pararenal space with luminal extension of lesion into IVC                                                                                        | Heteroechoic lesion in the retroperitoneum, in the right sub hepatic region filling and distending the hepatic and intrahepatic IVC                                                                                    | Heteroechoic lesion in the right sub hepatic location.                                                                                                                                                                                                          | Heteroechoic lesion involving right suprarenal location with extension to lumen of IVC.                                                                               | Hypoechoic lesion in the paraaortic location filling the lumen of IVC                                                                                                                       |
| MDCT                                       | Heterogeneously enhancing soft tissue density lesion with necrosis epicentred in the anterior pararenal space of retroperitoneum measuring 17.7 x 12.5 cm x 16.5cm, with a component extending into and distending the lumen of middle segment of IVC. | Heterogeneously enhancing lesion filling the luminal aspect of IVC with extraluminal component measuring 2.5 X 3.8 x 2.7 cm.                                                                             | Heterogeneously enhancing lobulated soft tissue density lesion with areas of necrosis filling the lumen of middle segment of IVC causing its distension and compressing right renal vein measuring 6.9 x 5.6 x 5.8 cm. | Lobulated heterogeneously enhancing soft tissue density lesion measuring 8.7 x 13.5 x 13.7 cm in the right side of retroperitoneum with areas of necrosis; the lesion was involving hepatic, suprarenal and infrarenal IVC, with extension to right renal vein. | Heterogeneously enhancing lesion in the right suprarenal location measuring 2.7 x 4.2 x 3.6 cm with extension of the lesion into the suprarenal segment of IVC        | Heterogeneously enhancing soft tissue density lesion with necrosis in the intraluminal compartment of IVC with extraluminal extension of middle segment of IVC measuring 4.5 x 3.2 x 3.4 cm |
| Involved IVC segment                       | Middle segment of IVC                                                                                                                                                                                                                                  | Middle segment of inferior vena                                                                                                                                                                          | Middle segment of IVC                                                                                                                                                                                                  | Upper, Middle and lower segment of IVC                                                                                                                                                                                                                          | Middle segment of IVC                                                                                                                                                 | Middle segment of IVC                                                                                                                                                                       |
| Extra luminal extension/ organ involvement | Hepatic and lung metastasis                                                                                                                                                                                                                            | Well defined small extraluminal component without infiltration of adjacent organs.                                                                                                                       | In the sub hepatic location with ill-defined fat planes with adjacent liver, infiltrating into lumen of suprarenal IVC, extensive deposits in mesentery and nodules in lung.                                           | Intraluminal extension up to the iliac vein and extraluminal to right lobe of liver and right kidney                                                                                                                                                            | Nil                                                                                                                                                                   | Extraluminal component of lesion having well defined fat planes with adjacent structures                                                                                                    |
| Management                                 | USG guided biopsy showing atypical spindle cell neoplasm with smooth muscle differentiation consistent with leiomyosarcoma: Inoperable -palliative care with chemotherapy                                                                              | IVC excision of tumour with reconstruction of vein. Histopathological analysis showed atypical spindle cell neoplasm with smooth muscle differentiation, SMA positive and MIB labelling index around 90% | USG guided biopsy showing atypical spindle cell neoplasm with smooth muscle differentiation. Inoperable-chemotherapy                                                                                                   | USG guided biopsy showing spindle cell neoplasm. Inoperable-chemotherapy.                                                                                                                                                                                       | IVC excision of tumour with reconstruction of vein. Histopathological analysis showed atypical spindle cell neoplasm with smooth muscle differentiation, SMA positive | USG guided biopsy showing spindle cell neoplasm. Chemotherapy                                                                                                                               |

**Table 1. Demographics, Clinical and Imaging Features of Subjects Diagnosed with IVC Leiomyosarcoma**



**Figure 4.** A 47-year-old male presented to our hospital with complaints of lower abdominal pain of one-month duration associated with loss of weight, bilateral lower limb oedema associated with loss of weight, bilateral lower limb oedema: coronal contrast enhanced computed tomography of abdomen showing heterogeneously enhancing lesion involving the middle and inferior segments of IVC (black arrow) with extraluminal component of the lesion (white arrow) in the sub hepatic location

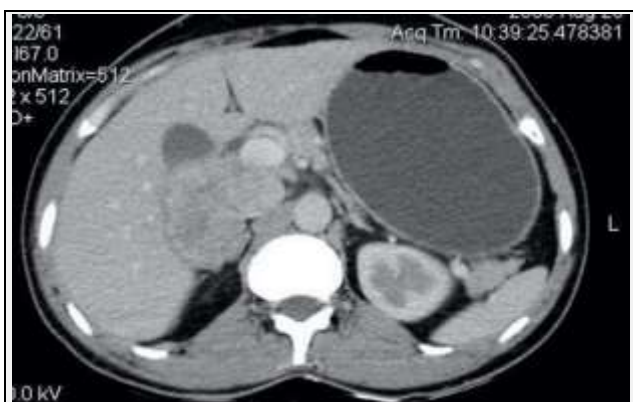


**Figure 5.** A 35-year-old female presented with chief complaints of upper abdominal pain and bilateral pedal oedema. On physical examination she had bilateral pedal oedema. axial contrast enhanced computed tomography of abdomen showing an enhancing lesion involving the suprarenal IVC distending its lumen.



**Figure 6.** A 64-year-old female with comorbidities of coronary artery disease, hypertension, and diabetes, complained of right abdominal discomfort of 2 months' duration and bilateral pedal oedema. Axial contrast enhanced computed tomography of abdomen shows a lesion within lumen of the middle segment of IVC (black arrow) with a component extending outside (white arrow).

**Case 1**

A 48-year-old female was presented to our hospital with complaints of right sided abdominal pain. On physical examination, a large mass was palpable in the right lumbar and epigastric region. Ultrasound evaluation of abdomen showed a large sub hepatic mass extending to retroperitoneum showing both intraluminal component in the hepatic IVC and the extraluminal component.

For further characterisation of the lesion, contrast enhanced computed tomography of abdomen was performed, which showed the lesion extending to inferior vena cava distending its lumen with a large sub hepatic extraluminal component (figure 1). The lung fields bilaterally showed focal nodules of varying sizes.

She underwent USG guided biopsy of the lesion. Histopathology was consistent with atypical spindle cell neoplasm with smooth muscle differentiation, myxoid changes with SMA positive and MIB labelling index around 90 %, a diagnosis of leiomyosarcoma was made.

**Case 2**

A 38-year-old female complaining of abdominal pain of 2 months duration. Local physical examination revealed no significant abnormality.

On routine ultrasound evaluation, a well-defined hetero-echoic lesion was detected in the right anterior pararenal space, in the region of head of pancreas with intraluminal extension into infrahepatic IVC (figure 2a).

Further evaluation with contrast enhanced computed tomography of abdomen showed a heterogeneously enhancing lesion at the level of pancreas in the anterior pararenal space with extension into lumen of inferior vena cava (figures 2b). She underwent IVC excision of tumour with interposition of graft repair of IVC using 14 mm coated polyester graft-right renal vein reimplantation polyester graft bypass to left renal vein.

Histopathology report was consistent with leiomyosarcoma.

**Case 3**

A 55-year-old male complaining of right sided abdominal pain, vague abdominal mass and bilateral pedal oedema for a duration of one month. Physical examination revealed pallor, a vague mass palpable in the right hypochondrium.

Ultrasound evaluation with curvilinear probe in the right hypochondrium showed a hetero-echoic lesion in the right sub hepatic location with lost fat planes within the liver.

Evaluation of the lesion by contrast enhanced computed tomography revealed heterogeneously enhancing lobulated lesion with ill-defined borders in the right suprarenal location, abutting the right kidney and infiltrating the right lobe of liver. Coronal sections confirmed the that the epicentre of the lesion was in the lumen of middle segment of inferior vena cava with a large extraluminal component showing infiltration of adjacent structures (figure 3). Further his lung fields showed few nodules and right pleural effusion.

She underwent USG guided biopsy of the lesion and the histopathology was consistent with leiomyosarcoma. Since

the tumour was extensive at the time of diagnosis with infiltration of adjacent structures and distant metastasis, she was offered with palliative chemotherapy.

#### Case 4

A 47-year-old male presented to our hospital with complaints of lower abdominal pain of one-month duration associated with loss of weight and physical examination revealed mild pallor and bilateral pitting pedal oedema.

On routine USG evaluation, a hetero-echoic lesion was detected in the right sub hepatic location with few hyperechoic foci within, having well-defined planes with right lobe of liver.

Contrast enhanced computed tomography of abdomen showed a well-defined hypodense lesion with few hyperdense foci, corresponding to calcification in the right suprarenal location. Coronal sections demonstrated the enhancing lesion to be in the lumen the middle and inferior segments of IVC with a large extraluminal component in the sub hepatic location (figures 4).

Ultrasound guided biopsy revealed atypical spindle cell neoplasm with smooth muscle differentiation, consistent with leiomyosarcoma. He was offered chemotherapy.

#### Case 5

A 35-year-old female presented with chief complaints of upper abdominal pain. On physical examination she had bilateral pedal oedema.

Routine ultrasound evaluation of abdomen revealed a lesion in the right hypochondrium.

For further characterisation of lesion, she was referred for MDCT abdomen which showed an enhancing lesion involving the suprarenal IVC distending its lumen (figure 5).

She underwent surgery with excision of the tumour with graft repair of the IVC. Histopathology was consistent with leiomyosarcoma.

#### Case 6

A 64-year-old female with co morbidities of coronary artery disease, hypertension and diabetes complaints of right abdominal discomfort for 2 months duration. On examination, bilateral pedal oedema was present.

Ultrasound evaluation showed a well-defined hypoechoic lesion involving the IVC in the paraaortic location.

Axial contrast CT sections of abdomen shows the lesion within lumen of the middle segment of IVC (black arrow) with a component extending outside (white arrow) (figure 6). Ultrasound guided biopsy showed features consistent with leiomyosarcoma. She was treated palliatively with chemotherapy, in view of co morbidities and lack of cooperation by her relatives for surgery.

for sarcomas, attributing to about 12 - 69 % of cases. It is the second most common tumour of the sarcomas affecting the retroperitoneum.<sup>2</sup> Primary vascular LMS is a rare entity of which, inferior vena cava (IVC) is the most common site.<sup>5</sup> Leiomyosarcoma of the inferior vena cava, described in fewer than 300 patients in the literature, is a rare clinical scenario.<sup>4</sup>

It is a slow growing tumour, and being located in the retroperitoneal space, symptoms are mostly non-specific and are identified incidentally once they are large enough to cause mass effect on adjacent structures.<sup>6</sup>

It is usually diagnosed with imaging modalities like computed tomography, magnetic resonance imaging, alone or in combination with ultrasonography, echocardiography. Thus, it becomes challenging due to its non-specific and wide varying clinical presentation, often preceding the diagnosis by months or years.<sup>5</sup> LMS of the IVC often are detected incidentally and are quite large at the time of diagnosis. In several studies, tumours were > 10 cm. In our study the average size of tumour detected was 9.3 cm.<sup>7</sup>

As per Teixeira et al. it most commonly affects females in the sixth decade. Occasionally, LMS of the IVC occurs in young patients, with few or no comorbidities, as localized disease.

In our study also, the majority affected were females.

The three major growth patterns described are extraluminal 62 %, intraluminal 5 % and combined 33 %. Based on the localisation along the IVC, these tumours can be further classified as involving the upper segment, spanning between hepatic veins to IVC, middle segment between the hepatic veins and renal veins and lower segment including the IVC below the renal veins.<sup>4</sup>

As per Yadav et al. LMS of IVC most frequently affects the middle segment, as is seen in our case.

Clinical presentation mainly depends on location, and is seen to be non-specific, which includes lower limb oedema, abdomen pain, mass, back pain, renal hypertension, and dyspnoea.

The most common route of metastasis is haematogenous, and is frequently to liver, lung bone, and brain. In advanced stages, the tumour may spread through lymphatics. In our case series we have found that two cases had metastasis at the time of diagnosis, and the preferentially involved site was lungs.

Leiomyosarcoma is a slow growing hypovascular tumour, sometimes hypervascular, corresponding to the involved segment and supplying arteries. Sonography may detect the tumour as a mixed hypoechogenic mass in the retroperitoneum. Detection of luminal extension of lesion to IVC, may help in clinching the diagnosis, but with many limitations.

Radiological techniques play an important role in the accurate diagnosis of LMS, particularly with cross sectional imaging modalities like CT or MRI. It can delineate an irregular-shaped heterogeneous lobulated soft-tissue mass in the IVC, expanding its lumen accompanied with peripheral post contrast enhancement and non-enhanced necrotic or cystic areas.<sup>8</sup>

## DISCUSSION

Leiomyosarcomas are mesenchymal neoplasms of smooth muscle cell origin.<sup>1</sup> Retroperitoneum is a common location

Leiomyosarcoma with predominant extraluminal component can be challenging to differentiate from other retroperitoneal tumours compressing the inferior vena cava.

As per Quian et al. among the differentials of intraluminal mass of IVC, includes leiomyosarcoma, angiosarcoma, tumour thrombus and bland thrombus.

The definitive diagnosis can be made only by USG or CT guided biopsy. The primary modality of treatment is surgery, and its resectability is determined by the location of the tumour, with those in the lower segment being completely resectable.

Surgery is currently the only potentially curative therapy.<sup>9</sup> Combination of radical resection of tumour with adjuvant chemotherapy is the treatment of choice for disease without metastasis at the time of diagnosis. The aim when approaching IVC LMS include achieving local control, maintaining the patency of major venous flow.<sup>10</sup> Though resistant to chemotherapy or radiotherapy, neoadjuvant therapy may be provided to downsize the tumour, prior undertaking surgical procedure.

### CONCLUSIONS

Leiomyosarcoma of IVC is a rare tumour, often detected late in the course due to its indolent manifestation. However, imaging done for non-specific complaints, is probably the only way to catch this lesion at its inception, offering best possible surgical cure preserving adjacent vital organs.

Data sharing statement provided by the authors is available with the full text of this article at jebmh.com.

Financial or other competing interests: None.

Disclosure forms provided by the authors are available with the full text of this article at jebmh.com.

### REFERENCES

- [1] Saphien A, Mousa MS, Bui MM, et al. Leiomyosarcoma of the inferior vena cava with hepatic and pulmonary metastases: Case report. *J Radiol Case Rep* 2019;13(5):30-40.
- [2] Marko J, Wolfman DJ. Retroperitoneal leiomyosarcoma. *Radiographics* 2018;38(5):1403-1420.
- [3] Kapoor R, Bansal A, Sharma SC. Leiomyosarcoma of inferior vena cava: case series of four patients. *J Cancer Res Ther* 2015;11(3):650.
- [4] Cortecero JM, Rubio MDG, Romá AP. Leiomyosarcoma of the inferior vena cava: AIRP best cases in radiologic-pathologic correlation. *Radiographics* 2015;35(2):616-620. <http://dx.doi.org/10.1148/rg.352130105>
- [5] Sessa B, Iannicelli E, Caterino S, et al. Imaging of leiomyosarcoma of the inferior vena cava: comparison of 2 cases and review of the literature. *Cancer Imaging* 2010;10(1):80-84.
- [6] Yadav R, Kataria K, Mathur S, et al. Leiomyosarcoma of inferior vena cava: a case series of four cases. *Indian J Pathol Microbiol* 2012;55(1):83.
- [7] Nascif RL, Antón AGS, Fernandes GL, et al. Leiomyosarcoma of the inferior vena cava: a case report. *Radiol Bras* 2014;47(6):384-386.
- [8] Teixeira FJR Jr, do Couto NSD, de Freitas PAL, et al. Leiomyosarcoma of the inferior vena cava: survival rate following radical resection. *Oncol Lett* 2017;14(4):3909-3916.
- [9] Tameo MN, Calligaro KD, Antin L, et al. Primary leiomyosarcoma of the inferior vena cava: reports of infrarenal and suprahepatic caval involvement. *J Vasc Surg* 2010;51(1):221-224.
- [10] Singla B, Bansal A. An insight into the inferior vena cava leiomyosarcoma. *Niger J Surg Sci* 2014;24(1):18-22.

RESEARCH

Open Access



# Hippocampal magnetic resonance imaging in focal onset seizure with impaired awareness—descriptive study from tertiary care centre in southern part of India

Aleena Elizabeth Andrews<sup>1</sup>, Naufal Perumpalath<sup>2</sup>, Juvaina Puthiyakam<sup>2</sup> and Andrews Mekkattukunnel<sup>3,4\*</sup>

## Abstract

**Background:** Temporal lobe epilepsy is the most common type of focal onset seizure. Focal onset seizure with impaired awareness, previously known as complex partial seizure (CPS), account for 18–40% of all seizure types. Hippocampal sclerosis (HS) is the most common cause of temporal lobe epilepsy, which produces focal onset seizure with impaired awareness. It may be detected in MRI visually, but bilateral abnormalities are better identified using volumetric analysis.

We aimed to compare hippocampal volume in patients with focal onset seizure with impaired awareness visually and quantitatively.

**Methodology:** This cross-sectional study includes clinically diagnosed cases of 56 focal onset seizure with impaired awareness undergoing MRI at a tertiary teaching hospital in the southern part of India for a duration of 18 months from February 2018 to August 2019.

**Results:** Out of 53 patients studied using 1.5 T MRI brain with seizure protocols, hippocampal atrophy was identified visually in 13 (24.5%) on the right side, 9 (16.98%) on the left side, and in 6 (11.32%) bilaterally. However, with volumetry, hippocampal atrophy (not taking T2 signal change) was detected in 15 (28.30%) on the right side, 10 (18.86%) on the left side, and in 7 (13.20%) bilaterally. Hippocampal volumes between ipsilateral and contralateral seizure focus were found to have no significant difference ( $p=0.84$ ).

**Conclusions:** Though visual analysis is efficient in the diagnosis of pathology, MR volumetry may be used as an expert eye in cases of subtle volume loss.

**Keywords:** Focal onset seizure with impaired awareness, Complex partial seizures, Mesial temporal lobe epilepsy (MTLE), Hippocampal sclerosis (HS), Hippocampal volumetry

\* Correspondence: [anjulioness@gmail.com](mailto:anjulioness@gmail.com)

<sup>3</sup>Professor of Medicine, Government Medical College Thrissur, Thrissur, Kerala 680002, India

<sup>4</sup>Mekkattukunnel House, Chakkoth lane, Poonkunnam, Thrissur, Kerala 680002, India

Full list of author information is available at the end of the article



© The Author(s). 2021 **Open Access** This article is licensed under a Creative Commons Attribution 4.0 International License, which permits use, sharing, adaptation, distribution and reproduction in any medium or format, as long as you give appropriate credit to the original author(s) and the source, provide a link to the Creative Commons licence, and indicate if changes were made. The images or other third party material in this article are included in the article's Creative Commons licence, unless indicated otherwise in a credit line to the material. If material is not included in the article's Creative Commons licence and your intended use is not permitted by statutory regulation or exceeds the permitted use, you will need to obtain permission directly from the copyright holder. To view a copy of this licence, visit <http://creativecommons.org/licenses/by/4.0/>.

## Background

Epilepsy is characterized by tendency to have recurrent seizures [1] with prevalence of 0.5–1%. Focal onset seizure with impaired awareness account for 18–40% of seizure types [2]. Focal onset seizure with impaired awareness can be of temporal and extra-temporal origin. The commonest form of temporal lobe epilepsy (TLE) is mesial temporal sclerosis where the pathology lies in hippocampus. TLE is responsible for two third cases of intractable epilepsy which is managed neurosurgically [3]. Most of the patients have good outcomes after surgery, and this depends on the evaluation by EEG and magnetic resonance imaging (MRI). Hippocampal sclerosis (HS) can be detected by visual inspection in most cases; however, volumetry can assist visual inspection if [3, 4] volume loss is subtle or bilateral resulting in lack of asymmetry, when the head is tilted while positioning in gantry or centres lack an expert in epilepsy imaging.

Many MR imaging studies interpreted as normal were later found to have hippocampal atrophy (HA) at tertiary epilepsy program [4]. There is a strong association between hippocampal asymmetry, identified by quantitative MR imaging, and visual inspection of the volumetric MR studies by two neuroradiologists who are trained to detect HA (91–97%) [4]. Thus, volumetric MR imaging can serve as an expert “eye”.

The mean volume of hippocampus is significantly smaller as compared to western population as well as northern regions of India, suggesting demographic variation in the hippocampal volume [5]. Very few data exist regarding the role of qualitative and quantitative hippocampal magnetic resonance imaging assessment in complex partial seizures from southern parts of the country.

## Methods

This cross-sectional study was conducted among all clinically diagnosed cases of focal onset seizure with impaired awareness, referred for MRI brain with seizure protocol in 2500-bedded tertiary care hospital from Southern India for a duration of 18 months from February 2018 to August 2019. The study included eligible cases diagnosed by senior neurologist using semiological and EEG criteria as per the International League Against Epilepsy (ILAE) 2017 guidelines [6]. The study was approved by the Institutional Review Board of the tertiary teaching hospital on 26 October 2017. As this imaging evaluation is a routine part of management of epilepsy, the written consent was waived by the ethics committee. The research involved no more than minimal risk to subjects and waiver will not adversely affect the rights and welfare of the subjects.

MR imaging was performed on 1.5 T MRI scanner (Wipro GE Healthcare, closed type with bore size of 60 cm, maximum amplitude of 33mT/m, USA in origin);

T1W, T2W, diffusion-weighted, and GRE sequences were obtained in axial plane with 5 mm slice thickness and 30% interslice gap. For dedicated hippocampal study, 3D T1w FSPGR (fast spoiled gradient echo sequence; inversion recovery prep) oblique coronal images (*TE* 5.8, *TR* 12.9, *FOV* 180 mm, *slice thickness* 3 mm *without interslice gap*, *matrix* 288 × 128 {*FE XPE* }, *NEX* -0.75, *phase FOV* 1, *prep time* 400 ms, *flip angle* 20, *bandwidth* of 15.63), T2W FLAIR coronal oblique images (*TE*: 95, *TR*: 8000, *FOV*: 160 mm, *slice thickness*: 3 mm), and oblique coronal T2W images (*TR*: 3700, *TE*: 97, *FOV*: 160, *slice thickness*: 6 mm) covering the whole brain were acquired. Oblique coronal plane was perpendicular to the long axis of the hippocampus.

Visually, hippocampus was assessed in T2W images for size and signal intensity. All MRIs were assessed for regional atrophy independently by 2 radiologists, blinded to all clinical details except age. The two radiologists had almost perfect agreement on evaluation of hippocampal atrophy visually ( $\kappa = 0.8373$ ).

The volume of the hippocampus was obtained from oblique coronal 3D T1w FSPGR sequences. Cross-sectional areas of both the hippocampi were measured in these oblique coronal sections by tracing hippocampal boundary manually from the hippocampal head to the tail. On MRI, the anterior-most boundary of the hippocampal head area is taken when the CSF in the uncus recess of the temporal horn was visible and is considered as the most reliable boundary between the hippocampal head and the amygdala. If uncus recess was not visible, then the alveus was used. To standardize the measurement, first section of the anterior hippocampus was defined as the point where the uncus recess or alveus first appears. Posterior margin of hippocampal volumetric measurement was defined by MR image where the crus of fornix were seen in full profile. Lateral and medial borders were defined as CSF in the temporal horn of the lateral ventricle and CSF in the uncus/ambient cisterns, respectively. Inferior border was defined by grey-white matter junction between the subiculum and white matter of the parahippocampal gyrus. The volumes of both hippocampi were calculated by summing each of the cross-sectional volumes {cross sectional area × (section thickness + interslice gap)}. As per study conducted by Mohandas, Aravind Narayan and colleagues on normative data of hippocampal volumetry Indian population, a mean hippocampal volume was found to be 2.411 cm<sup>3</sup> [5]. This was much smaller as compared to the data available from the western population.

Statistical analysis was performed using percentages and proportions for qualitative data (visual assessment of hippocampal volume). Quantitative data (volumetry and T2 relaxometry of hippocampus) are presented as mean with standard deviation. The statistical significance

of differences in mean volumes between right and left sides were assessed using the 't' test.

Values that are 2 SD below the mean of normal and left–right asymmetries at least 2 SD above or below the mean of normal are taken as abnormal for individual patients.

All analysis was done using epi info 7 version software (CDC open software, in Atlanta, GA, USA) and Microsoft Excel. Pearson's correlation coefficient and t test were used wherever indicated. p value < 0.05 was considered to be significant.

Initially visual assessment of the sections of the brain was performed, in which those cases without space occupying lesions/perilesional oedema involving hippocampus ( $n = 53$ ) were assessed visually and subjected to volumetry using specific sequences (oblique coronal T2 FLAIR, oblique coronal three-dimensional T1w FSPGR).

## Results

There were 56 patients in the study with a mean age of 26.44 with SD 14.78 years (see Fig. 1).

By the Shapiro-Wilk test of normality, it was found that the data differed significantly from normal distribution (test statistic 0.856; df 56; p value is 0.000). Age, gender, and febrile seizure distribution is depicted in Table 1.

Fifty-six patients with TLE were further divided into right TLE and left TLE groups based on the side of EEG localization. Six patients (10.71%) whose seizure foci were either outside the temporal lobe or had a

multifocal origin or could not be localized were grouped as extratemporal/unclassified (ET/UC).

Out of 56 patients evaluated with MRI, 13 patients (23.21%) had mesial temporal sclerosis, seven had tumours, one had non-specific white matter T2 hyperintensity in the extratemporal location, 12 had hippocampal atrophy without signal alteration, 1 had T2 hyperintensity of the hippocampus without volume loss, and 22 (39.28%) had no obvious abnormalities in imaging with 1.5 T MRI. Three cases with perilesional oedema due to tumour extending into the hippocampus were excluded from analysis (see Fig. 1).

The major tumours detected were glioblastoma multiforme ( $n = 2$ ), dysembryoplastic neuroectodermal tumour ( $n = 3$ ), ganglioglioma ( $n = 1$ ), and glioma ( $n = 1$ ).

Using visual assessment, atrophy with T2 hyperintensity of the hippocampus was seen in 9 (16.98%) on the right side, 5 on the left side (9.4%), and bilaterally in 1 (1.9%) only (Table 2).

Hippocampal atrophy with T2 hyperintensity suggestive of sclerosis (see Fig. 2) was seen in 9 (16.98%) on the right side; however, there was a single case of T2 hyperintensity without atrophy.

In our study out of 53 cases, 13 cases (24.5%) showed atrophy of mammillary bodies/fornix with temporal horn dilation ipsilateral to the side of the hippocampal atrophy. In the cases where there was bilateral hippocampal atrophy, it was seen that there was atrophy of either mammillary body or fornix and temporal horn dilation visually in both sides (see Fig. 3).

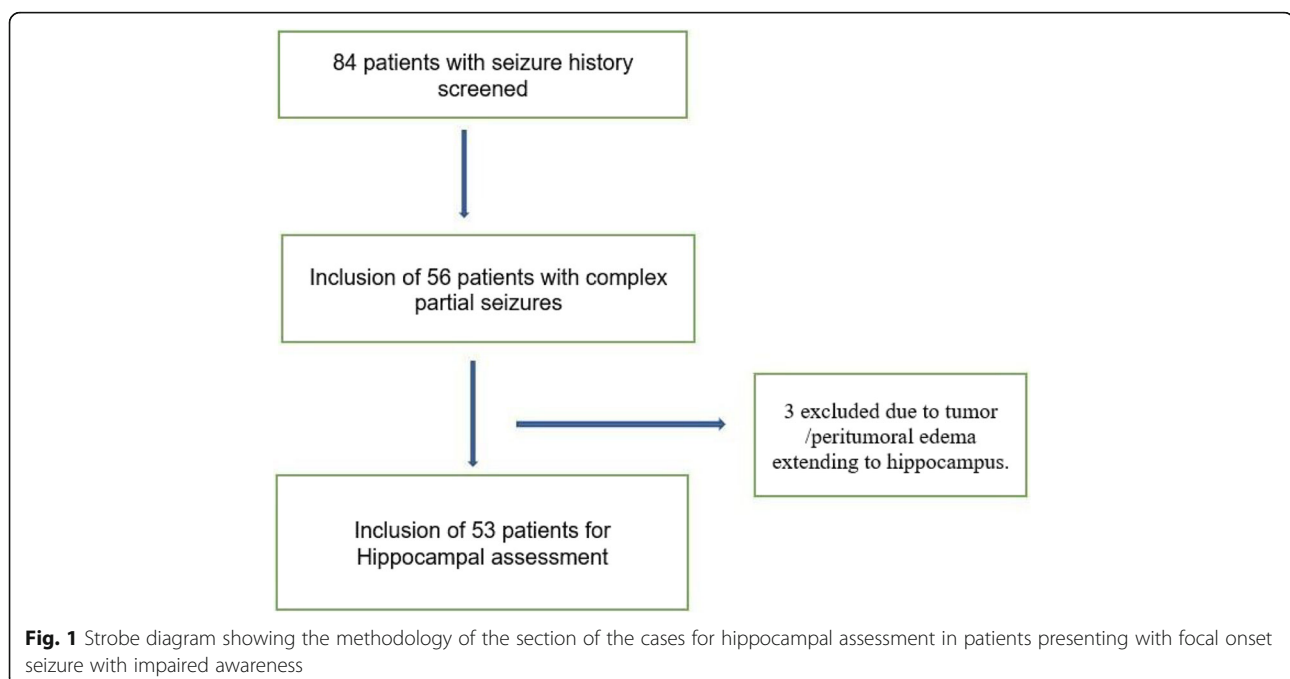


**Table 1** Age, gender, and presence of febrile seizures in patients with complex partial seizure (focal onset seizures with impaired awareness)

| Gender | Number     | Median Age with SD | Febrile Seizure |
|--------|------------|--------------------|-----------------|
| Male   | 30(53.57%) | 22(15.99)          | 13(43.33%)      |
| Female | 26(46.43%) | 19.5(13.40)        | 6(23.36%)       |

To label hippocampal atrophy, a cut off value of 2.4 cc was taken [4].

Among the 53 cases, 15 (28.30%) had right-sided atrophy quantitatively (not taking T2 hyperintensity into consideration), 10 (18.87%) had left sided atrophy, and 7 (13.20%) had bilateral atrophy.

Combining hippocampal atrophy with signal alteration in T2, 7 had right hippocampal sclerosis, 4 had left hippocampal sclerosis, and 2 had bilateral hippocampal sclerosis (see Fig. 4).

Comparisons of right and left hippocampal volumes on ipsilateral and contralateral to seizure focus revealed no significant difference ( $n = 53$ , mean volume right – 2.54, left 2.56  $p$ -0.80).

Comparing the T2 relaxometry of the hippocampus in presumed normal cases and those with hippocampal sclerosis on either side showed a statistically significant difference (Table 3).

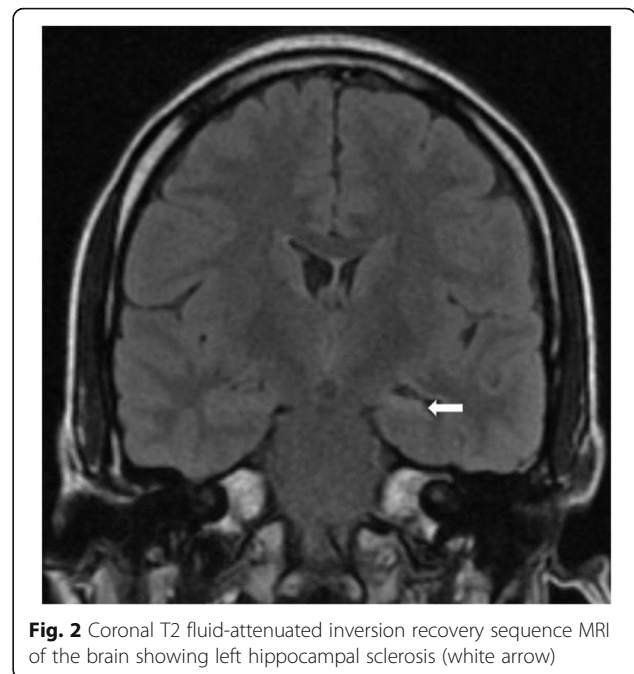
Comparisons of right and left hippocampal T2 relaxometry values ipsilateral and contralateral to seizure focus were analysed and were found to have no statistically significant difference ( $n = 53$ , mean 81.44 on the right, 86 on the left and  $p$ -0.86).

## Discussion

As per estimate, 1% of the world population suffers from epilepsy, of which the most common adult type is focal onset seizure with impaired awareness (previously known as complex partial seizure) [7]. Williamson PD, French JA, Thadani VM, Kim JH, and colleagues noted that more than 80% cause of TLE is mesial temporal lobe sclerosis (MTS) [8]. But in our study, 23.21% showed features suggestive of MTS, seven had tumours, one had non-specific white matter T2 hyperintensity in extratemporal location, 12 had hippocampal atrophy

**Table 2** Hippocampal atrophy and T2 hyperintensity distribution in CPS (focal onset seizures with impaired awareness)

|                                   | Right       | Left       | Bilateral  |
|-----------------------------------|-------------|------------|------------|
| Atrophy                           | 13 (24.53%) | 9 (16.98%) | 6 (11.32%) |
| T2 hyperintensity                 | 10 (18.87%) | 6 (11.32%) | 1 (1.9%)   |
| Atrophy with T2 hyperintensity    | 9 (16.98%)  | 5 (9.4%)   | 1 (1.9%)   |
| T2 hyperintensity without atrophy | 1 (1.9%)    | 0          | 0          |

**Fig. 2** Coronal T2 fluid-attenuated inversion recovery sequence MRI of the brain showing left hippocampal sclerosis (white arrow)

without signal alteration, and 1 had T2 hyperintensity of hippocampus without volume loss.

The major tumours detected in our study were glioblastoma multiforme ( $n = 2$ ), dysembryoplastic neuroectodermal tumour ( $n = 3$ ), ganglioglioma ( $n = 1$ ), and glioma ( $n = 1$ ). As per study by Brooks and colleagues, tumours were detected in 22% subjects [9].

In our study, 22 subjects (39.28%) had no obvious abnormalities in imaging with 1.5 T MRI. As per Muhlhofer W, Tan Y-L, Mueller SG, and Knowlton R, up to 30% of TLE cases have normal (“non lesional” or negative) magnetic resonance imaging (MRI) [10].

Magnetic resonance imaging (MRI) features of hippocampal sclerosis (HS) by visual analysis of MRI as described by Cendes and colleagues are hippocampal atrophy, increased T2/FLAIR signal, loss of internal structure, asymmetry of the horns of the lateral ventricles, atrophy of the anterior temporal lobe, and atrophy of the ipsilateral fornix and mammillary bodies [11].

Classical imaging findings in hippocampal sclerosis include volume loss and increased signal intensity in T2/FLAIR images [12]. Increased signal intensity of hippocampus with atrophy visually was found in 13 (24.53%) patients on the right side and 9(16.98%) in patients on the left side. Six out of 53 cases had bilateral hippocampal atrophy without corresponding increase in signal intensity in T2.

Atrophy is the most specific and reliable feature of hippocampal sclerosis (HS) [13].

The significance of extent of atrophy of hippocampus becomes important in assessing the prognosis after surgery for mesial temporal sclerosis. In a study by Kim y

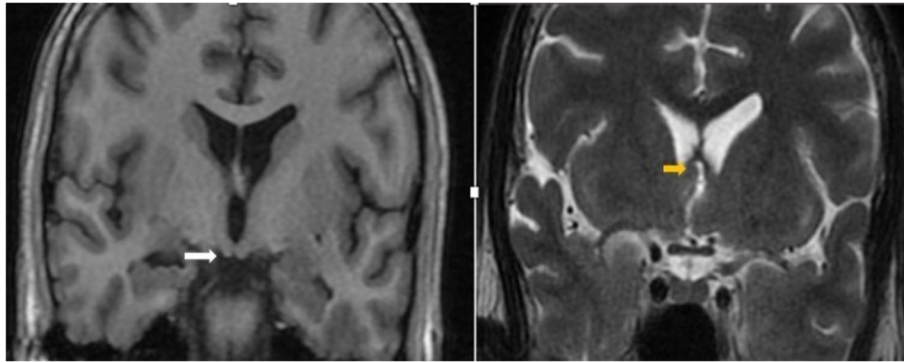


**Fig. 3** Coronal MRI of brain showing mammillary body atrophy on the right side (white arrow) and right fornix atrophy (yellow arrow) in the patient with focal onset seizure with impaired awareness

and colleagues, it was seen that an MR imaging finding of hippocampal atrophy is the most useful sole prognostic indicator [13].

Visual identification of abnormal hippocampus is straightforward if one side is clearly normal and the other is abnormal. In symmetric bilateral disease or mild unilateral disease, visual analysis may produce problems [11].

The secondary findings in the mammillary bodies and fornix on MR imaging help in the diagnosis and lateralization of MTS [14]. In our study out of 53 cases, 13 cases showed atrophy of mammillary bodies/fornix with temporal horn dilation ipsilateral to the side of hippocampal atrophy.

In patients with subtle findings of unilateral MTS, the secondary imaging features may add to improve diagnostic confidence. Although the secondary MR imaging findings associated with MTS are not sensitive predictors of this entity by themselves, they may offer clues in subtle cases [15].

Quantitative hippocampal volumetry has been shown to predict postsurgical outcome in various studies; however, according to Kim y and colleagues, the interpretation of MR images by visual inspection alone has a similar prognostic value [12].

Quantitatively, 15 (28.30%) subjects had hippocampal atrophy volumetrically vs. 13 (24.53%) visually on the right side, whereas on the left side, only 9 (16.98%)

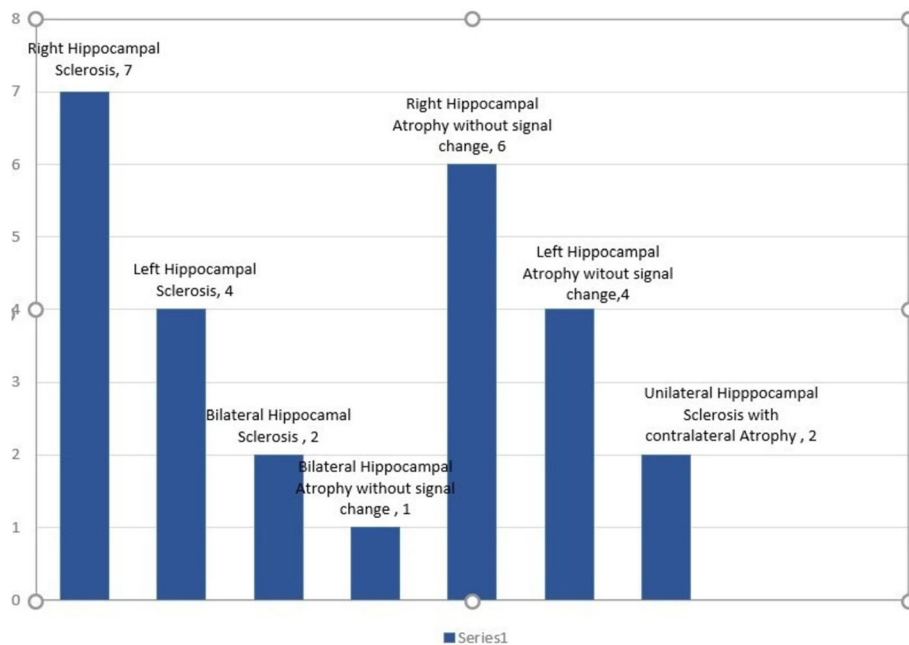


**Fig. 4** Distribution of hippocampal atrophy with T2 hyperintensity in patients with focal onset seizure with impaired awareness

**Table 3** Mean T2 relaxometry of hippocampal sclerosis in comparison with normal hippocampus in patients with focal onset seizures with impaired awareness

| Side  | Normal | Hippocampal sclerosis | p value         |
|-------|--------|-----------------------|-----------------|
| Right | 71.32  | 81.44                 | 0.008 (t-2.482) |
| Left  | 76.13  | 86                    | 0.048 (t-1.725) |

subjects were detected visually, while 10 (18.87%) were detected volumetrically to have atrophy. In our study, by volumetry, we were able to detect more cases of atrophy quantitatively which was not evident on visual inspection alone.

Another important indicator of hippocampal sclerosis is increased hippocampal T2 signal which indicates gliosis [13]. The degree and extent of hippocampal gliosis also correlate with the T2 signal in the hippocampus.

MR imaging studies by Bronen RA, Jackson GD, and colleagues have described a variable frequency of T2 signal change in the hippocampus: change was observed in 12 to 65% of patients with hippocampal sclerosis [13].

But in our study, T2 hyperintensity were found in 30.18%. In our study, there is a single case with T2 hyperintensity of hippocampus ipsilateral to the clinical and EEG localisation of the seizure focus (right sided), however with no atrophy.

As per study by Kim y and colleagues, it has been suggested that finding of hippocampal atrophy is more useful than one of high T2 signal in determining hippocampal sclerosis by histology. As per Kim and colleagues, hippocampal atrophy was much more common finding than high T2 signal (97% vs. 61%).

T<sub>2</sub>-weighted hyperintensity is one of the salient radiologic features of HS which can be objectively assessed by quantitative measurement of T2 relaxation (T2 mapping). It has got higher sensitivity over visual analysis. It is of great importance to note that T2 values may be elevated even in the absence of atrophy [16]. Thus, the combination of hippocampal atrophy with an elevated T2 value is both sensitive and specific for HS. As a result, combining findings of hippocampal volumes and T2 values can increase the yield to 99% of visually detected HS, but also 28% of those considered visually normal [1].

In our study, comparisons of the right and left hippocampal T2 relaxometry values in subjects with normal and abnormal hippocampus were found to have a statistically significant difference.

Jackson G. D and colleagues performed hippocampal T2 relaxometry as routine MRI examination and concluded that abnormal T2 relaxometry is significantly associated with intractable epilepsy [17].

## Conclusion

Visual inspection alone may be sufficient to diagnose hippocampal sclerosis, but in cases with subtle volume

loss or bilateral atrophy, volumetry serves as an expert eye. Secondary signs such as atrophy of mammillary body, fornix, and prominence of the temporal horn of the lateral ventricle are of paramount significance while assessing the hippocampal atrophy visually especially if the pathology is bilateral.

T2 relaxometry turns out to be a useful tool in detecting hippocampal sclerosis, as a striking difference is noted in cases with hippocampal sclerosis and those presumed to have normal hippocampus.

## Limitation

1. MTS accounts for the majority of the cases of focal onset seizure with impaired awareness (CPS), and hence MRI is done to confirm the diagnosis as a pre-operative work-up. However, since surgery for hippocampal sclerosis is not performed in our institution, most of the patients suspected with hippocampal sclerosis are referred to centres where surgery is performed and evaluated with MRI there.
2. Limited sample size.
3. The results of T2 relaxometry is equipment specific, and therefore, variations may occur based on the equipment used for evaluation.
4. The study has not considered the frequency of seizure episodes in assessing the hippocampal atrophy.

## Abbreviations

CPS: Complex partial seizures; ILAE: The International League Against Epilepsy; HS: Hippocampal sclerosis; MRI: Magnetic resonance imaging; MTS: Mesial temporal sclerosis; TLE: Temporal lobe epilepsy

## Acknowledgements

We are grateful to the neurology department and the senior neurologist for referring the cases for MRI. We are grateful to the technologists/radiographers for acquiring the MRI images according to seizure protocol.

## Authors' contributions

The corresponding author MA and first author AEA chose the idea and put the proposal. The first author AEA is the principal investigator, researched the literature and conceived the study, and was involved in protocol development, gaining of ethical approval, and data collection and analysis. The second author NP and third author JP were the two senior readers/observers who analysed the MRI. The corresponding author MA helped the first author AEA in the drafting of the manuscript. All authors reviewed and edited the manuscript and approved the final version of the manuscript.

## Funding

This research required no external funding from any agency. The entire expense was met by the principal investigator.

## Availability of data and materials

The data used and analysed in this study are available from the authors on reasonable request.

## Declarations

### Ethics approval and consent to participate

This work has been accepted by the institutional research and ethics committee of Government Medical College, Kozhikode (Calicut), on 26 October 2017 (reference number GMCKKD/RP 2017/EC/176). Consent to participate has been approved also by the same committee.

### Consent for publication

Not applicable

### Competing interests

The authors have no conflict of interests.

### Author details

<sup>1</sup>Department of Radiodiagnosis, Government Medical College, Thrissur, Kerala, India. <sup>2</sup>Department of Radiodiagnosis, Government Medical College Kozhikode, Kozhikode, India. <sup>3</sup>Professor of Medicine, Government Medical College Thrissur, Thrissur, Kerala 680002, India. <sup>4</sup>Mekkattukunnel House, Chakkoth lane, Poonkunnam, Thrissur, Kerala 680002, India.

Received: 7 April 2021 Accepted: 25 June 2021

Published online: 23 July 2021

## References

- Singh P, Kaur R, Saggar K, Singh G, Kaur A. Qualitative and quantitative hippocampal MRI assessments in intractable epilepsy. *Biomed Res Int*. 2013; 2013:480524.
- Kramer U, Riviello JJ Jr, Carmant L, Black PM, Madsen J, Holmes GL. Clinical characteristics of complex partial seizures: a temporal versus a frontal lobe onset. *Seizure*. 1997;6(1):57–61. [https://doi.org/10.1016/S1059-1311\(97\)80054-4](https://doi.org/10.1016/S1059-1311(97)80054-4).
- Vos SB, Winston GP, Goodkin O, Pemberton HG, Barkhof F, Prados F, et al. Hippocampal profiling: localized magnetic resonance imaging volumetry and T2 relaxometry for hippocampal sclerosis. *Epilepsia*. 2020;61(2):297–309. <https://doi.org/10.1111/epi.16416>.
- Farid N, Girard HM, Kemmotsu N, Smith ME, Magda SW, Lim WY, et al. Temporal lobe epilepsy: quantitative MR volumetry in detection of hippocampal atrophy. *Radiology*. 2012;264(2):542–50. <https://doi.org/10.1148/radiol.12112638>.
- Mohandas AN, Bharath RD, Prathyusha PV, Gupta AK. Hippocampal volumetry: normative data in the Indian population. *Ann Indian Acad Neurol*. 2014;17(3):267–71. <https://doi.org/10.4103/0972-2327.138482>.
- Fisher RS, Cross JH, D'Souza C, French JA, Haut SR, Higurashi N, et al. Instruction manual for the ILAE 2017 operational classification of seizure types. *Epilepsia*. 2017;58(4):531–42. <https://doi.org/10.1111/epi.13671>.
- Owolabi L, Sale S, Owolabi S. Clinico-electroencephalography pattern and determinant of 2-year seizure control in patients with complex partial seizure disorder in Kano, Northwestern Nigeria. *Ann Med Health Sci Res*. 2014;4(2):186–91. <https://doi.org/10.4103/2141-9248.129030>.
- Williamson PD, French JA, Thadani VM, Kim JH, Novelly RA, Spencer SS, et al. Characteristics of medial temporal lobe epilepsy: II. Interictal and ictal scalp electroencephalography, neuropsychological testing, neuroimaging, surgical results, and pathology. *Ann Neurol*. 1993;34(6):781–7. <https://doi.org/10.1002/ana.410340605>.
- Brooks BS, King DW, el Gammal T, Meador K, Yaghmai F, Gay JN, et al. MR imaging in patients with intractable complex partial epileptic seizures. *AJNR Am J Neuroradiol*. 1990;11(1):93–9.
- Muhlhofer W, Tan YL, Mueller SG, Knowlton R. MRI-negative temporal lobe epilepsy—What do we know? *Epilepsia*. 2017;58(5):727–42. <https://doi.org/10.1111/epi.13699>.
- Cendes F, Theodore WH, Brinkmann BH, Sulc V, Cascino GD. Neuroimaging of epilepsy. *Handb Clin Neurol*. 2016;136:985–1014. <https://doi.org/10.1016/B978-0-444-53486-6.00051-X>.
- Dou W, Zhao L, Su C, Lu Q, Liu Q, Guo J, et al. A quantitative MRI index for assessing the severity of hippocampal sclerosis in temporal lobe epilepsy. *BMC Med Imaging*. 2020;20(1):42. <https://doi.org/10.1186/s12880-020-00440-z>.
- Kim YH, Chang KH, Park SW, Koh YW, Lee SH, Yu IK, et al. Hippocampal sclerosis: correlation of MR imaging findings with surgical outcome. *Korean J Radiol*. 2001;2(2):63–7. <https://doi.org/10.3348/kjr.2001.2.2.63>.
- Bote RP, Blázquez-Llorca L, Fernández-Gil MA, Alonso-Nanclares L, Muñoz A, De Felipe J. Hippocampal sclerosis: histopathology substrate and magnetic resonance imaging. *Semin Ultrasound CT MR*. 2008;29(1):2–14. <https://doi.org/10.1053/j.sult.2007.11.005>.
- Kuzniecky R, de la Sayette V, Ethier R, Melanson D, Andermann F, Berkovic S, et al. Magnetic resonance imaging in temporal lobe epilepsy: pathological correlations. *Ann Neurol*. 1987;22(3):341–7. <https://doi.org/10.1002/ana.410220310>.
- Winston GP, Vos SB, Burdett JL, Cardoso MJ, Ourselin S, Duncan JS. Automated T2 relaxometry of the hippocampus for temporal lobe epilepsy. *Epilepsia*. 2017;58(9):1645–52. <https://doi.org/10.1111/epi.13843>.
- Jackson GD, Connelly A, Duncan JS, Grünewald RA, Gadian DG. Detection of hippocampal pathology in intractable partial epilepsy: increased sensitivity with quantitative magnetic resonance T2 relaxometry. *Neurology*. 1993; 43(9):1793–9. <https://doi.org/10.1212/WNL.43.9.1793>.

## Publisher's Note

Springer Nature remains neutral with regard to jurisdictional claims in published maps and institutional affiliations.

**Submit your manuscript to a SpringerOpen<sup>®</sup> journal and benefit from:**

- Convenient online submission
- Rigorous peer review
- Open access: articles freely available online
- High visibility within the field
- Retaining the copyright to your article

Submit your next manuscript at ► [springeropen.com](https://www.springeropen.com)

# Histopathological Correlation of Time Signal Intensity Curve in MRI Detected Breast Lesions

Juvaina. P<sup>1\*</sup>, Gomathy Subramaniam<sup>2</sup>, V.R. Rajendran<sup>2</sup>, P. Rajan<sup>2</sup>, Naufal. P<sup>3</sup>

<sup>1\*</sup>Assistant Professor, <sup>2</sup>Professor, <sup>3</sup>Associate Professor,  
Department of Radiodiagnosis, Government Medical College, Kozhikode, Kerala, India.

## ABSTRACT

**Introduction:** Dynamic contrast enhanced MR imaging of breast characterizes the lesions more accurately than morphological parameters which helps in to distinguish between benign and malignant lesions.

**Aims:** To differentiate benign from malignant breast lesions detected on MRI by analyzing quantitative lesion characteristics. To compare and correlate the radiological diagnosis with the final histopathological diagnosis.

**Materials and Methods:** A prospective study on 41 cases was conducted in the department of Radiodiagnosis, Government Medical College, Kozhikode during the period from Aug 2009 to July 2010 who were undergoing MRI of breast for characterization of lesions. Contrast enhancement Initial and post initial kinetics were plotted on a graph to get the time signal intensity curve which was studied and correlated with the final histopathological diagnosis.

**Results:** Of the total 41 cases, 48.8% were malignant and 51.2% were benign. 38.1% of the benign lesions showed <50% initial enhancement while no malignant lesions showed this. 80% of malignancies demonstrated strong (>100%) initial enhancement. 20% of malignant lesions and 28.6% of benign lesions demonstrated moderate (50-100%) initial enhancement. Continuous post initial kinetics was noted in

66.7% of benign lesions and none of the malignant lesions. 95% of malignancies showed washout kinetics. Plateau kinetics was shown by 5% of malignant and 9.5% of benign lesions

**Conclusion:** Malignant lesions more frequently showed >100% initial kinetics and type III (wash out) post initial kinetics; however, an overlap exists.

**Keywords:** Breast MRI, Breast Lesion, Time Signal Intensity Curve, Initial Kinetics, Post Initial Kinetics, Benign, Malignant.

## \*Correspondence to:

**Dr. Juvaina.P,**  
Assistant Professor, Department of Radiodiagnosis,  
Government Medical College, Kozhikode, Kerala, India.

## Article History:

Received: 22-03-2017, Revised: 20-04-2017, Accepted: 25-04-2017

## Access this article online

|                                                              |                                                                                                              |
|--------------------------------------------------------------|--------------------------------------------------------------------------------------------------------------|
| Website:<br><a href="http://www.ijmrp.com">www.ijmrp.com</a> | Quick Response code<br> |
| DOI:<br>10.21276/ijmrp.2017.3.3.015                          |                                                                                                              |

## INTRODUCTION

Contrast enhanced MR imaging of breast characterizes the lesions more accurately than mammography or sonography. Dynamic contrast enhanced MR imaging of breast lesions characterizes the lesions more accurately than morphological parameters which helps in to distinguish between benign and malignant lesions.

## AIMS AND OBJECTIVES

1. To differentiate benign from malignant breast lesions that had been detected on MR imaging by analyzing its contrast enhancement initial and post initial kinetics.
2. To compare and correlate the radiological diagnosis with the final histopathological diagnosis

## MATERIALS AND METHODS

### Study Design

Diagnostic test evaluation

## Study Setting

All patients undergoing MR imaging of breast at Department of Radiodiagnosis, Govt. Medical College, Kozhikode for characterization of breast lesions detected clinically, by x-ray mammography or by ultrasonography.

## Study Period

August 2009 to July 2010

## Study Method

41 cases of breast lesions were evaluated with MRI. Dynamic parameters like contrast enhancement initial and post initial kinetics studied and plotted on a graph to get the time signal intensity curve which was studied and correlated with the final histopathological diagnosis. Final histopathological report of all the lesions were compared and correlated with MRI findings

The following criteria's were evaluated.

Kinetic data was evaluated by visually assessing the lesion enhancement pattern by placing a region of interest to obtain

kinetic curves and by using a computer aided detector system. ROIs placed with wide window settings into the area that exhibits strongest enhancement on the first post contrast image.<sup>1</sup> Enhancement dynamics describes the signal intensity changes occurring in a contrast enhancing region with respect to time.<sup>2</sup> To quantify enhancement, the increase in signal intensity relative to base line pre contrast signal intensity is measured.<sup>1</sup> The initial signal increase (in %) is the maximum signal intensity within the first 2 minutes after contrast medium administration compared to signal intensity of the pre contrast image. It is calculated using the formula.<sup>2</sup>

**Initial Signal Increase (%) =**  

$$\frac{\text{Signal (post cm)} - \text{Signal (pre cm)} \times 100}{\text{Signal (pre cm)}}$$
 [cm = contrast measurement]

**Initial Signal Increase**

None to slight: Less than 50% increase in signal intensity compared to pre contrast measurement.

Moderate: Between 50% and 100% increase in signal intensity compared to pre contrast measurement.

Strong: Over 100% increase in signal intensity compared to pre contrast measurement.

**Post Initial Signal Behaviour<sup>2</sup>**

This describes the course of signal curve between 2-8 minutes after contrast administration.

**Post initial signal behaviour =**

$$\frac{\text{Signal (8mts)} - \text{Signal (max 1 - 2 mts)} \times 100\%}{\text{Signal (max1-2mts)}}$$

Three types of time signal intensity curves have been described.<sup>3,4</sup>

- (i) **Type I (Continuous):** Signal increase over 10%
- (ii) **Type II (Plateau):** Constant signal intensity (+/- 10%)
- (iii) **Type III (Washout):** Signal decrease over 10%

**Sample Size**

41 patients  
 All patients satisfying inclusion criteria were included in the study.

**Inclusion Criteria**

- a) Patients with inconclusive study by mammogram or ultrasound.
- b) Those which have biopsy proven malignancy.
- c) Those which have cytology proven malignancy with benign appearance of lesion by mammogram or ultrasound.
- d) Post-operative or post chemotherapy patients to know residual disease.
- e) Those with occult carcinoma with breast primary in axillary lymph node

**Exclusion Criteria**

- 1. Patients under hormone therapy
- 2. Patients in luteal phase of menstrual cycle
- 3. Patients with contraindication for MRI.

**MRI Protocols and Imaging (Technique Used)**

MRI was performed on a 1.5 T commercial available system (signaHDxT, General Electric Health care), bilateral 8 channel phased array breast coil. Images were acquired with the patient in prone position and with both breasts imaged simultaneously & the following sequences were performed.

- (a) Pre contrast T1 weighted fat suppressed 3D fast spoiled gradient echo
- (b) Post contrast T1 W axial dynamic study after a rapid bolus injection of gadopentetate dimeglumine (0.1 mmol/kg of body weight) delivered through an indwelling IV catheter followed by 10ml saline bolus infusion.; the comprehensive dynamic protocol consisted of fast dynamic imaging in the first 45 seconds followed by slow dynamic imaging in 6 consecutive series at 78 seconds intervals.

After the examination, the unenhanced images were subtracted from the first enhanced images on a pixel by pixel basis.

**Statistical Analysis**

Statistical analysis was performed using computerized statistics software (Epi- Info, centres for Disease control and prevention, Atlanta, GA) with the Chi-square and Fischer's exact tests. Sensitivity, specificity and associated statistics were worked out and provided.

**Figure 1: Distribution according to contrast enhancement-initial kinetics**

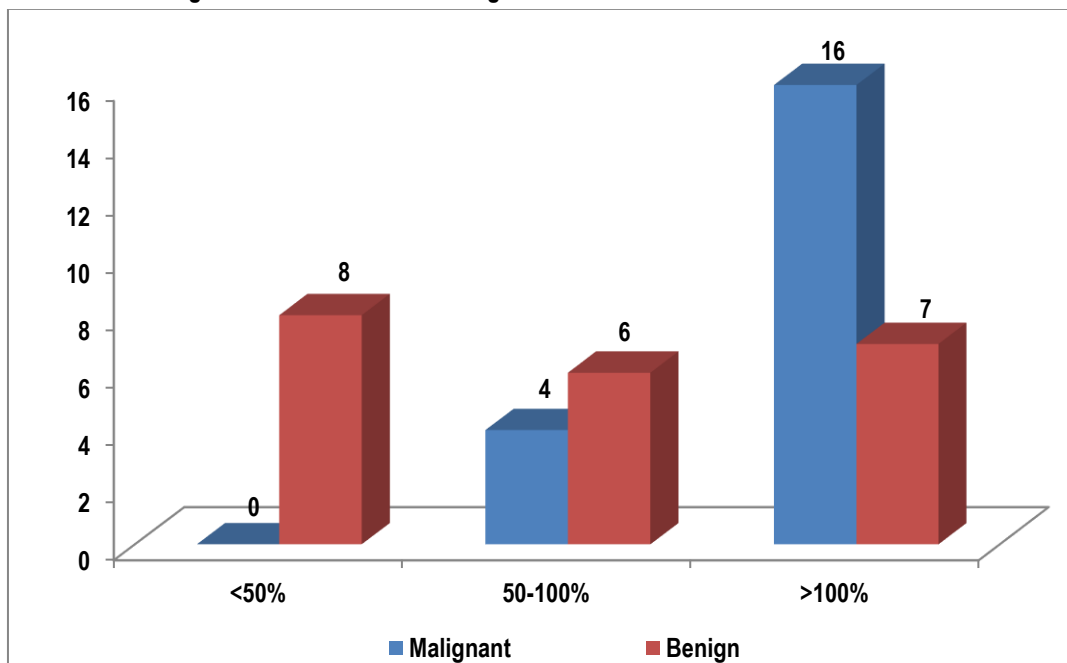


Figure 2: Distribution according to post initial kinetics

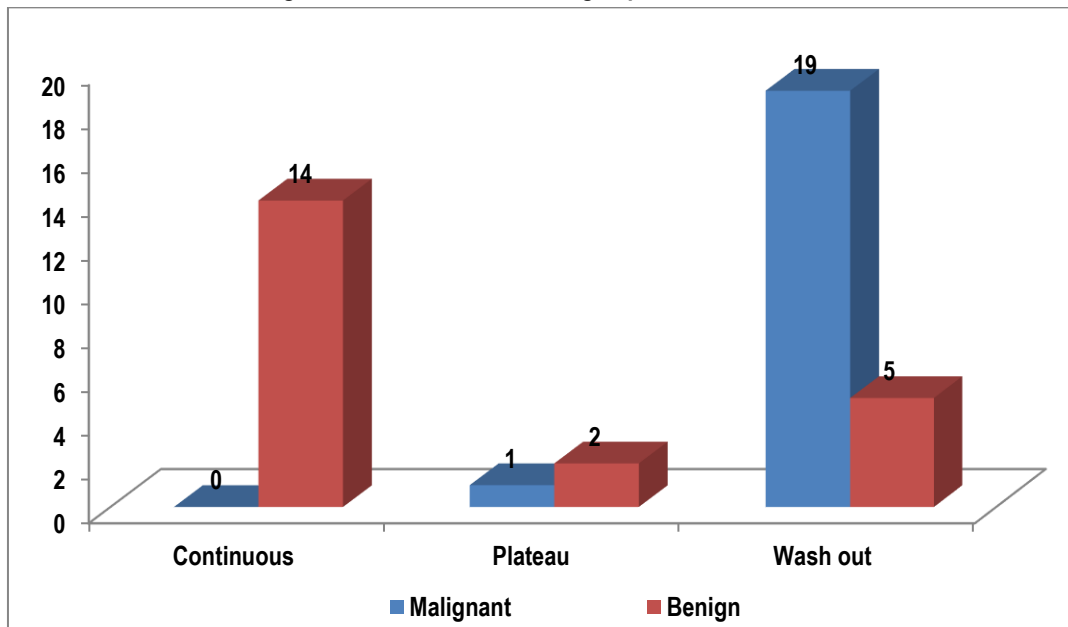


Table 1: Frequency distribution of initial kinetics <50%

| Test results | Gold standard diagnosis |        | Total |
|--------------|-------------------------|--------|-------|
|              | Malignant               | Benign |       |
| Positive     | 0                       | 8      | 8     |
| Negative     | 20                      | 13     | 33    |
| Total        | 20                      | 21     | 41    |

Table 2: Statistical indices of initial kinetics <50%

|                           |     |
|---------------------------|-----|
| Sensitivity               | 0%  |
| Specificity               | 62% |
| Positive predictive value | 0%  |
| Negative predictive value | 39% |

Table 3: Frequency distribution of initial kinetics 50-100%

| Test results | Gold standard diagnosis |        | Total |
|--------------|-------------------------|--------|-------|
|              | Malignant               | Benign |       |
| Positive     | 4                       | 6      | 10    |
| Negative     | 16                      | 15     | 31    |
| Total        | 20                      | 21     | 41    |

Table 4: Statistical indices of initial kinetics 50-100%

|                           |     |
|---------------------------|-----|
| Sensitivity               | 20% |
| Specificity               | 71% |
| Positive predictive value | 40% |
| Negative predictive value | 48% |

Table 5: Frequency distribution of initial kinetics >100%

| Test results | Gold standard diagnosis |        | Total |
|--------------|-------------------------|--------|-------|
|              | Malignant               | Benign |       |
| Positive     | 16                      | 7      | 23    |
| Negative     | 4                       | 14     | 18    |
| Total        | 20                      | 21     | 41    |

Table 6: Statistical indices of initial kinetics >100%

|                           |     |
|---------------------------|-----|
| Sensitivity               | 80% |
| Specificity               | 67% |
| Positive predictive value | 70% |
| Negative predictive value | 78% |

**Table 7: Frequency distribution of type I curve**

| Test results | Gold standard diagnosis |        | Total |
|--------------|-------------------------|--------|-------|
|              | Malignant               | Benign |       |
| Positive     | 0                       | 14     | 14    |
| Negative     | 20                      | 7      | 27    |
| Total        | 20                      | 21     | 41    |

**Table 8: Statistical indices of type I curve**

|                           |     |
|---------------------------|-----|
| Sensitivity               | 0%  |
| Specificity               | 33% |
| Positive predictive value | 0%  |
| Negative predictive value | 26% |

**Table 9: Frequency distribution of type II curve**

| Test results | Gold standard diagnosis |        | Total |
|--------------|-------------------------|--------|-------|
|              | Malignant               | Benign |       |
| Positive     | 1                       | 2      | 3     |
| Negative     | 19                      | 19     | 38    |
| Total        | 20                      | 21     | 41    |

**Table 10: Statistical indices of type II curve**

|                           |     |
|---------------------------|-----|
| Sensitivity               | 5%  |
| Specificity               | 90% |
| Positive predictive value | 33% |
| Negative predictive value | 50% |

**Table 11: Frequency distribution of type III curve**

| Test results | Gold standard diagnosis |        | Total |
|--------------|-------------------------|--------|-------|
|              | Malignant               | Benign |       |
| Positive     | 19                      | 5      | 24    |
| Negative     | 1                       | 16     | 17    |
| Total        | 20                      | 21     | 41    |

**Table 12: Statistical indices of type III curve**

|                           |     |
|---------------------------|-----|
| Sensitivity               | 95% |
| Specificity               | 76% |
| Positive predictive value | 79% |
| Negative predictive value | 94% |

## RESULTS

Of the total 21 benign lesions, <50% initial enhancement was observed in 38.1% while no malignant lesions showed this. Significant percentage (80%) of malignancies demonstrated strong (>100%) initial enhancement. 20% of malignant lesions and 28.6% of benign lesions demonstrated moderate (50-100%) initial enhancement. Continuous post initial kinetics was noted in 66.7% of benign lesions and none of the malignant lesions. 95% of malignancies showed washout kinetics. Plateau kinetics was shown by 5% of malignant and 9.5% of benign lesions.

Out of the four atypical ductal hyperplasia cases equal distribution was noted between moderate (50-100%) and strong (>100%) initial kinetics, also a similar pattern was observed in post initial dynamics (two showed plateau and two showed wash out curve).

Of the three papillomas, all showed type III (wash out) post initial kinetics with two showing >100% initial kinetics and one showing 50-100% initial kinetics. All the two sclerosing adenosis without atypia showed type I (continuous) post initial kinetics with both of them showing rapid initial enhancement. All the inflammatory changes (six) showed type I (continuous) post initial kinetics with four (66.6%) showing <50% and two (33.3%) showing 50-100% initial kinetics.

## DISCUSSION AND CONCLUSIONS

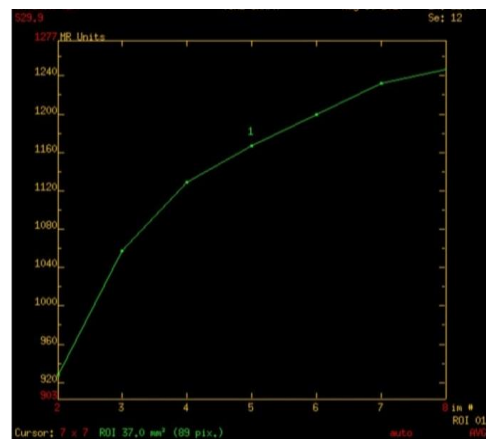
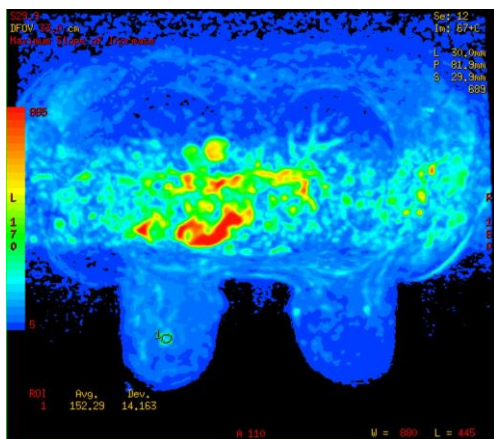
### Initial Dynamics

In this study, of the total 21 benign cases, <50% initial enhancement was observed in 38.1% while no malignant lesions showed this. Significant percentage (80%) of malignancies demonstrated strong (>100%) initial enhancement. 20% of malignant lesions and 28.6% of benign lesions demonstrated 50-100% initial enhancement.

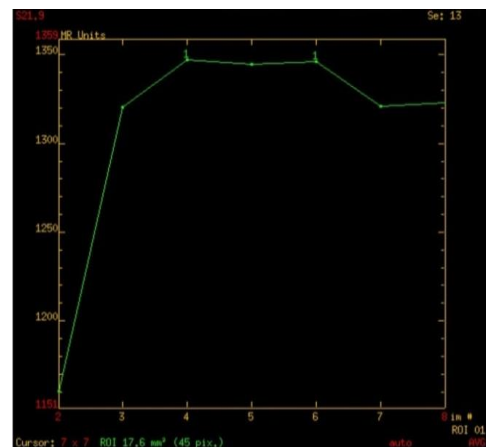
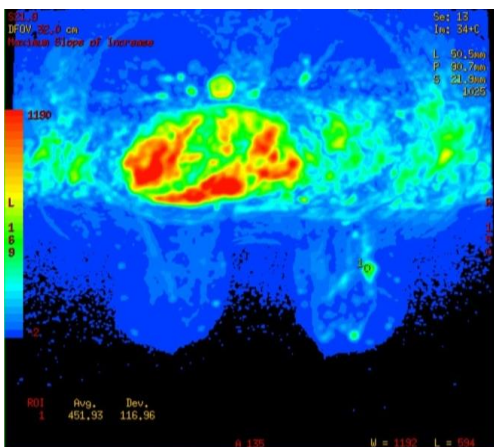
Schnall et al<sup>5</sup> concluded that the quantitative features most indicative of cancer were the maximum enhancement rate and the percentage of enhancement at 1 minute with rapid enhancement being characteristic of a malignancy which is well correlating with the present study. Siegmann et al<sup>6</sup> proposed that malignant lesions showed a higher maximum slope of the enhancement curve, reached the mean signal intensity peak earlier. Nevertheless there exists a considerable overlap. Kuhl et al<sup>3</sup> found that there was a considerable overlap in the range of enhancement rates of benign and malignant lesions with a reported sensitivity of 91%, a specificity of 37%, a positive predictive value of 47% and a NPV of 87%. The study observed that significant number (95%) of malignant lesions showed washout curve even though overlap existed. This correlates with

the study by Siegmann et al<sup>6</sup> who concluded that malignant lesions showed a stronger loss of enhancement (wash out) from

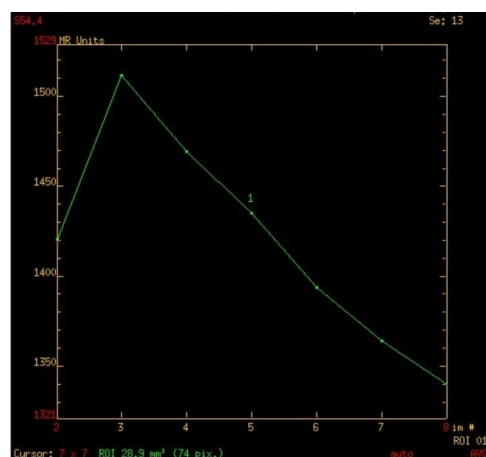
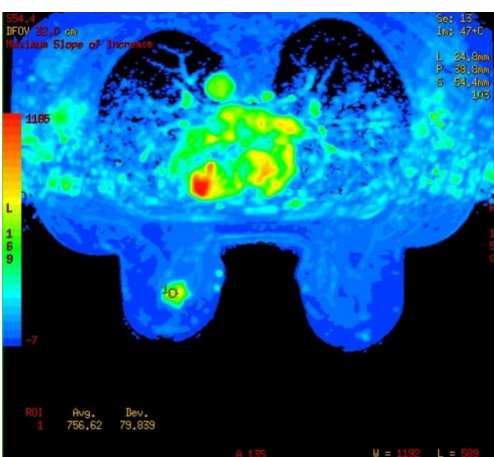
the initial signal intensity peak to the last contrast enhanced measurement. Nevertheless there exists a considerable overlap.



Case 1: Color coded map of the enhancing lesion in left breast with time signal intensity curve showing type I curve. HPR-Fibroadenoma



Case 2: Color coded map of the enhancing lesion in right breast with time signal intensity curve showing type II curve. HPR-Atypical ductal hyperplasia



Case 3: Color coded map of the enhancing lesion in left breast with time signal intensity curve showing type III curve. HPR- Invasive ductal carcinoma with ductal carcinoma in situ

Table 13: Post initial dynamics – Percentage distribution among benign and malignant lesions

|                             | Type I curve |           | Type III curve |           |
|-----------------------------|--------------|-----------|----------------|-----------|
|                             | Benign       | Malignant | Benign         | Malignant |
| Schnall et al <sup>5</sup>  | 45%          |           |                | 76%       |
| Kuhl et al <sup>3</sup>     | 83%          |           |                | 57%       |
| Liberman et al <sup>7</sup> |              |           |                | 33%       |
| Present study               | 66.7%        | 0%        | 23.8%          | 95%       |

The present study reports that 23.8% of benign lesions demonstrated washout curve. This disparity may be explained by the histologic variety of the lesions in this study. Benign lesions like sclerosing adenosis, atypical ductal hyperplasia, papillomas and young fibroadenomas showed washout kinetics.

Kuhl et al<sup>3</sup> reported that 83% of the benign lesion exhibited a steady continuous time signal intensity curve compared to 66.7% in the present study.

Liberma et al<sup>7</sup> found that the most common pattern was plateau present in 64%. Carcinoma was present in 33% of the lesions that showed wash out versus 24% of the lesions that had other kinetic

patterns. Infiltrating carcinoma was present in 29% of the lesions with wash out versus 6% of the lesions without wash out.

In this study, atypical ductal hyperplasia and papillomas demonstrated features favouring malignancy.

In papillomas the study observed malignant quantitative features like wash out kinetics (100%) and rapid initial enhancement (66.6%). In contrast, 50% of sclerosing adenosis without atypia showed benign post initial kinetics which is correlating with previous studies<sup>8</sup>. On reviewing pathology literatures<sup>9-11</sup>, both papillomas and atypical ductal hyperplasia have got an increased relative risk for subsequent development of malignancies.

**Table 14: Features of malignancy in benign lesions in the present study**

|                          | Atypical ductal hyperplasia | Papilloma  | Sclerosing adenosis without atypia |
|--------------------------|-----------------------------|------------|------------------------------------|
| <b>Wash out kinetics</b> | 50% (n=2)                   | 100% (n=3) | 0%                                 |

**REFERENCES**

1. Kuhl C. The current status of breast MR imaging. Choice of technique, image interpretation, diagnostic accuracy and transfer to clinical practice. *Radiology* 2001; 244: 356-378.
2. Uwe Fischer, Practical MR mammography 2004, Thieme, Stuttgart. Newyork. *Radiology* 2001; 244: 356-378.
3. Kuhl CK, Mielcareck P, Klaschik S, et al Dynamic breast MR imaging: Area signal intensity time course data useful for differential diagnosis of enhancing lesions? *Radiology* 211: 101-110, 1999.
4. Kuhl CK, Schild HH: Dynamic image interpretation of MRI of breast. *J Magn Reason imaging* 12: 965-974, 200.
5. Schnall MD, Blume J, Bluemhe DA, etal Diagnostic architectural and dynamic features at breast MR imaging: multicenter study. *Radiology* 2006; 238: 42 – 53.
6. Siegmann KC, Muller – Schimpfle in Schick F.etal MR Imaging – Detected breast lesions: Histopathologic correlation of lesion characteristics and signal intensity data: *AJR* 2002,178:1403-09.
7. Liberman etal. Breast lesions detected on MR imaging: Features and positive predictive value. *AJR* 2002, 179: 171-178.
8. Heywang – Kobrunner SH, Beck R. Contrast enhanced MRI of the breast 2nd ed. Berlin: Springer – Verlag : 1996.
9. Fitz Gibbons PL, Page DL, Weaver D, Thor AD, All red DL, Chank GM, Ruby SG, O'Malley F, Simpson JF, Connolly JL, Hayes DF, Edge SB, Lichter A, Schnitt SJ. Prognostic factors in breast cancer. College of American Pathologists consensus statement 1997. *Arch Pathol Lab Med* 2000; 124: 966-978.

10. Jensen RA, Page BL, Dupont WD, Rogers LW, Invasive Breast Cancer risk in women with sclerosing adenosis. *Cancer* 1989, 64:1977-1983.
11. Fischer, Dorothee R, Waurdinges, Susanne, Boettes, Joachim, Matrich, Ansgar, Kaiser, Werner A. Further Signs in the Evaluation of Magnetic Resonance Mammography: A Retrospective Study. *Investigative Radiology* 2005 July; 40 (7); 430 – 435.

**Source of Support:** Nil.

**Conflict of Interest:** None Declared.

**Copyright:** © the author(s) and publisher. IJMRP is an official publication of Ibn Sina Academy of Medieval Medicine & Sciences, registered in 2001 under Indian Trusts Act, 1882. This is an open access article distributed under the terms of the Creative Commons Attribution Non-commercial License, which permits unrestricted non-commercial use, distribution, and reproduction in any medium, provided the original work is properly cited.

**Cite this article as:** Juvaina.P, Gomathy Subramaniam, V.R. Rajendran, P.Rajan, Naufal.P. Histopathological Correlation of Time Signal Intensity Curve in MRI Detected Breast Lesions. *Int J Med Res Prof.* 2017; 3(3):70-75.  
DOI:10.21276/ijmrp.2017.3.3.015

## MR IMAGING DETECTED BREAST LESIONS- HISTOPATHOLOGICAL CORRELATION OF QUALITATIVE LESION CHARACTERISTICS

Juvaina Puthiyakam<sup>1</sup>, Gomathy Subramaniam<sup>2</sup>, V. R. Rajendran<sup>3</sup>, Rajan P<sup>4</sup>, Naufal P<sup>5</sup>, Saanida M. P.<sup>6</sup>, Jineesh T<sup>7</sup>, Soumya Hareendranath<sup>8</sup>

<sup>1</sup>Assistant Professor, Department of Radiodiagnosis, Government Medical College, Kozhikode.

<sup>2</sup>Professor, Department of Radiodiagnosis, Government Medical College, Kozhikode.

<sup>3</sup>Professor and HOD, Department of Radiodiagnosis, Government Medical College, Kozhikode.

<sup>4</sup>Professor, Department of Radiodiagnosis, Government Medical College, Kozhikode.

<sup>5</sup>Associate Professor, Department of Radiodiagnosis, Government Medical College, Kozhikode.

<sup>6</sup>Assistant Professor, Department of Radiodiagnosis, Government Medical College, Kozhikode.

<sup>7</sup>Assistant Professor, Department of Radiodiagnosis, Government Medical College, Kozhikode.

<sup>8</sup>Assistant Professor, Department of Radiodiagnosis, Government Medical College, Kozhikode.

### ABSTRACT

#### BACKGROUND

Contrast-enhanced MR imaging of breast characterises the lesion more accurately than mammography or sonography. This contributes to the distinction between benign and malignant lesions. Multifocal and contralateral lesions can also be better detected by MR imaging.

Aims- To differentiate benign from malignant breast lesions that have been detected on MRI by analysing qualitative lesion characteristics. To compare and correlate the radiological diagnosis with the final histopathological diagnosis.

#### MATERIALS AND METHODS

A prospective study on 41 cases was conducted in the Department of Radiodiagnosis, Govt. Medical College, Kozhikode during the period of Aug. 2009 to July 2010 who were undergoing MR imaging of breast for characterisation of lesions. Morphological parameters of the lesions were correlated with the final histopathological diagnosis.

#### RESULTS

66.6% of benign lesions showed well-defined (Oval, round, lobulated) shape while none of the malignant lesions demonstrated this. Irregular shape was observed in all the malignancies. Smooth margin was observed in 66.7% of benign lesions while ill-defined margin like irregular & spiculated constituted 70% and 25% respectively in malignancies. None of the malignant lesions showed smooth margin.

#### CONCLUSION

Well-defined shape and smooth margin were characteristic of benign lesions. Spiculated margin was highly specific for malignancy. Both irregular and spiculated margin had a high predictive value for malignancy.

#### KEYWORDS

MRI, Breast Lesion, Shape, Margin, Benign, Malignant.

**HOW TO CITE THIS ARTICLE:** Puthiyakam J, Subramaniam G, Rajendran VR, et al. MR imaging detected breast lesions- Histopathological correlation of qualitative lesion characteristics. J. Evolution Med. Dent. Sci. 2017;6(42):3284-3287, DOI: 10.14260/Jemds/2017/711

#### BACKGROUND

Contrast-enhanced MR imaging of breast characterises the lesions more accurately than mammography or sonography. This contributes to the distinction between benign and malignant lesions. Multifocal and contralateral lesions can also be better detected by MRI.

#### Aims and Objectives

1. To differentiate benign from malignant breast lesions that have been detected on MR imaging by analysing qualitative lesion characteristics.

*Financial or Other, Competing Interest: None.*

*Submission 23-03-2017, Peer Review 12-05-2017,*

*Acceptance 19-05-2017, Published 25-05-2017.*

*Corresponding Author:*

Juvaina Puthiyakam,

Assistant Professor,

Department Radiodiagnosis,

Government Medical College, Kozhikode.

E-mail: juvaina.faiz@gmail.com

DOI: 10.14260/jemds/2017/711



2. To compare and correlate the radiological diagnosis with the final histopathological diagnosis.

#### MATERIALS AND METHODS

##### Study Design

Descriptive study; Diagnostic test evaluation.

##### Study Setting

All patients undergoing MR imaging of breast at Dept. of Radiodiagnosis, Govt. Medical College, Kozhikode for characterisation of breast lesions detected clinically, by x-ray mammography or by ultrasonography.

##### Study Period

August 2009 to July 2010

##### Study Method

41 cases of breast lesions were evaluated with MRI. Morphologic parameters like shape and margin were studied. Final histopathological report of all the lesions were compared and correlated with MRI findings.

**The Following Criteria were evaluated-**

1. Shape - well defined (Round, oval, lobulated).
  - Irregular (Linear, branching, stellate)
2. Margin - Smooth/irregular/spiculated.

Histopathological diagnosis - Fibroadenoma/papilloma/atypical duct hyperplasia/invasive carcinoma with DCIS /Recurrent mass/inflammatory changes/sclerosing adenosis with no atypia.

**Sample Size**

41.

**Inclusion Criteria**

1. Patients with inconclusive study by mammogram or ultrasound.
2. Those which have biopsy proven malignancy.
3. Those which have cytology proven malignancy with benign appearance of lesion by mammogram or ultrasound.
4. Post-operative or post-chemotherapy patients to know residual disease.
5. Those with occult carcinoma with breast primary in axillary lymph node.

**Exclusion Criteria-**

1. Patients under hormone therapy.
2. Patients in luteal phase of menstrual cycle.
3. Patients with contraindication for MRI.

**MRI Protocols and Imaging**

MRI was performed on a 1.5 T commercial available system (Signa HDxT, General Electric Healthcare), bilateral 8-channel phased-array breast coil. Images were acquired with the patient in prone position and with both breasts imaged simultaneously & the following sequences were performed-

- (a) T1 W axial.
- (b) T2 W axial & sagittal with fat suppression.
- (c) Post contrast T1 W axial dynamic study.

**Statistical Analysis**

Statistical analysis was performed using computerised statistics software (Epi- Info, Centres for Disease Control and Prevention, Atlanta, GA) with the Chi-square and Fisher's exact tests. Sensitivity, specificity and associated statistics were worked out and provided.

**Ethics**

The study was approved by the institutional research committee and ethics committee of Government Medical College, Kozhikode, Kerala, India.

**RESULTS**

1. Shape- 66.6% of benign lesions showed well-defined (oval, round, lobulated) shape while none of the malignant lesions demonstrated this. However, irregular shape was observed in all the malignancies.

|                  | Malignant | Benign | TOTAL |
|------------------|-----------|--------|-------|
| <b>Oval</b>      | 0         | 5      | 5     |
|                  | 0%        | 23.8%  | 12.2% |
| <b>Round</b>     | 0         | 4      | 4     |
|                  | 0%        | 19%    | 9.8%  |
| <b>Lobulated</b> | 0         | 5      | 5     |
|                  | 0%        | 23.8%  | 12.2% |
| <b>Irregular</b> | 20        | 7      | 27    |
|                  | 100%      | 33.3%  | 65.9% |

**Table 1. Distribution According to Shape**

|                           |     |
|---------------------------|-----|
| Sensitivity               | 0%  |
| Specificity               | 76% |
| Positive predictive value | 0%  |
| Negative predictive value | 44% |

**Table 2. Statistical Indices of Oval Shape**

|                           |     |
|---------------------------|-----|
| Sensitivity               | 0%  |
| Specificity               | 81% |
| Positive predictive value | 0%  |
| Negative predictive value | 46% |

**Table 3. Statistical Indices of Round Shape**

|                           |     |
|---------------------------|-----|
| Sensitivity               | 0%  |
| Specificity               | 76% |
| Positive predictive value | 0%  |
| Negative predictive value | 44% |

**Table 4. Statistical Indices of Lobulated Shape**

|                           |      |
|---------------------------|------|
| Sensitivity               | 100% |
| Specificity               | 67%  |
| Positive predictive value | 74%  |
| Negative predictive value | 100% |

**Table 5. Statistical Indices of Irregular Shape**

2. Margin- Smooth margin was observed in 66.7% of benign lesions while ill-defined margin like irregular & spiculated constituted 70% and 25% respectively in malignancies with none of them showing smooth margin.

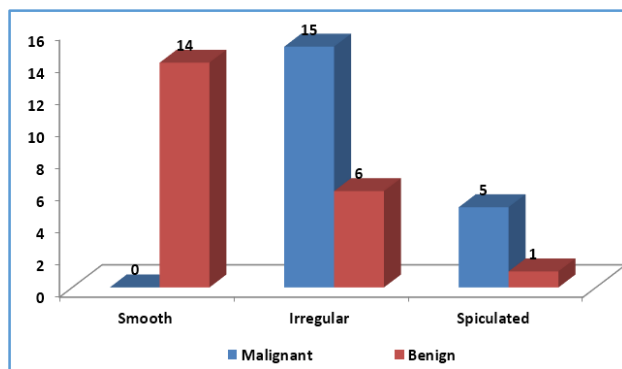


**Figure 1. Distribution According to Margin**

|                           |     |
|---------------------------|-----|
| Sensitivity               | 0%  |
| Specificity               | 33% |
| Positive predictive value | 0%  |
| Negative predictive value | 26% |

**Table 6. Statistical Indices of Smooth Margin**

|                           |     |
|---------------------------|-----|
| Sensitivity               | 75% |
| Specificity               | 71% |
| Positive predictive value | 71% |
| Negative predictive value | 75% |

**Table 7. Statistical Indices of Irregular Margin**

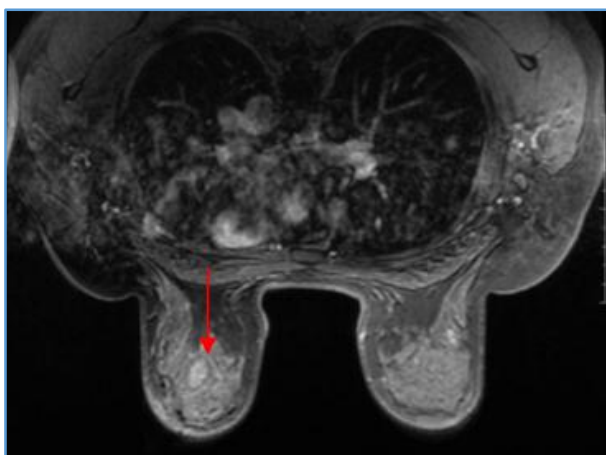
|                           |     |
|---------------------------|-----|
| Sensitivity               | 25% |
| Specificity               | 95% |
| Positive predictive value | 83% |
| Negative predictive value | 57% |

**Table 8. Statistical Indices of Spiculated Margin**

- All the six fibroadenomas were having well defined (oval, round or lobulated) shape with smooth margin.
- Of the four atypical duct hyperplasia, except one showing irregular shape and margin, rest were having round / lobulated shape with smooth margin.
- All the papillomas were having smooth margin with lobulated / oval shape.
- Of the two sclerosing adenosis without atypia, irregular and smooth margin as well as irregular and round shape was having equal distribution.

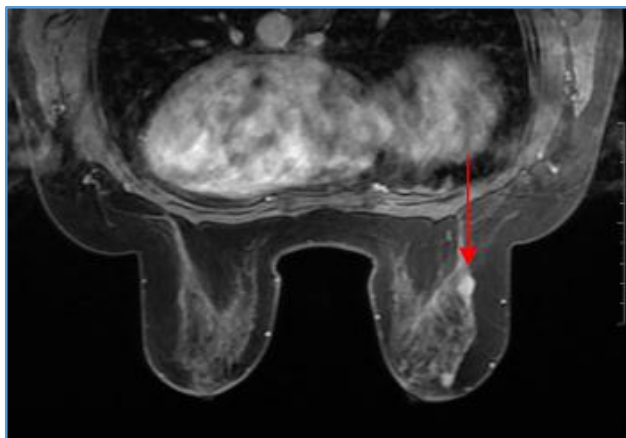
**Case 1**

Contrast-enhanced fat suppressed 3D FSPGR image showing well defined oval lesion with smooth margin in left breast. HPR-Fibroadenoma.



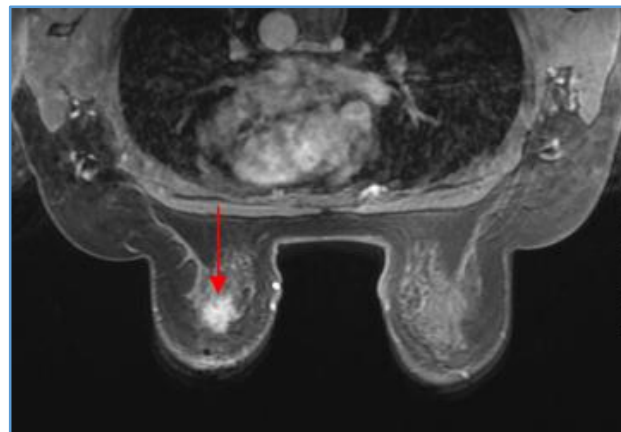
**Case 2**

Contrast-enhanced fat suppressed 3D FSPGR image showing well defined lobulated lesion with smooth margin in right breast. HPR-atypical ductal hyperplasia.



**Case 3**

Contrast-enhanced fat suppressed 3D FSPGR image showing irregular lesion with spiculated margin in left breast; HPR-invasive ductal carcinoma with ductal carcinoma in situ.



**DISCUSSION**

In this study, well-defined shape had a specificity of 75-80% in predicting benignity while irregular shape had a sensitivity and specificity of 100% and 67% for diagnosing malignancy respectively. Present study revealed a comparatively lower negative predictive value (NPV) for smooth margin since more of post-treatment cases with irregular margin were included. Also, this study categorised well-defined shape into oval, round and lobulated. So considering them as one group in previous studies might have increased the negative predictive values.

According to Nunes et al,<sup>1</sup> a typical benign feature for masses is a smooth margin (NPV of 95%). If a mass is lobulated and shows no enhancement or only minimal enhancement, it is likely to be benign (NPV of 100%).

Orel, Gilles, Hams et al<sup>2,3</sup> concluded from their study that one of the architectural features suggestive of benign process include a mass with smooth or lobulated borders.

|                   | Nunes et al <sup>4</sup> | Schnall et al <sup>5</sup> | Liberman et al <sup>6</sup> | Present Study |
|-------------------|--------------------------|----------------------------|-----------------------------|---------------|
| Irregular margin  | 81%                      | 84%                        | -                           | 71%           |
| Spiculated margin | 88%                      | 91%                        | 80%                         | 83%           |

**Table 9. Positive Predictive value**

In this study, ill-defined margin had a high positive predictive value for malignancy [71% for irregular & 83% for spiculated margin] which is well correlating with the study by Nunes et al.<sup>1</sup> They reported that irregular margin has a positive predictive value of 81% and spiculated margin has a positive predictive value of 88% for diagnosing malignancy.

Nunes, Schnall and Orel et al<sup>4</sup> also concluded that architectural features highly predictive of malignancy include spiculated borders (PPV for malignancy of 91%) and irregular borders (PPV for malignancy of 84%). This also correlates with the present study.

Liberman et al<sup>6</sup> concluded that the features with higher PPV were spiculated margins (80% of carcinoma) and irregular shape (32% carcinoma) for mass lesions which is well correlating with the present study.

Orel, Gilles, Hams et al<sup>2,3</sup> concluded from their study that one of the architectural features suggestive of malignancy include a mass with irregular or spiculated borders.

#### CONCLUSION

Well-defined shape and smooth margin were characteristic of benign lesions. Spiculated margin was highly specific for malignancy. Both irregular and spiculated margin had a high predictive value for malignancy.

#### REFERENCES

- [1] Nunes LW, Schnall MD, Siegelman ES, et al. Diagnostic performance characteristics of architectural features revealed by high spatial-resolution MR imaging of the breast. *AJR Am J Roentgenol* 1997;169(2):409-15.
- [2] Gilles R, Guinebretiere JM, Lucidarme O, et al. Nonpalpable breast tumors: diagnosis with contrast-enhanced subtraction dynamic MR imaging. *Radiology* 1994;191(3):625-31.
- [3] Hams SE, Flamig DP, Hensley KL, et al. MR imaging of the breast with rotating delivery of excitation off resonance: clinical experience with pathologic correlation. *Radiology* 1993;187(2):493-501.
- [4] Nunes LW, Schnall MD, Orel SG. Update of breast MR imaging architectural interpretation model. *Radiology* 2001;219(2):484-94.
- [5] Schnall MD, Roster S, Englander S, et al. A combined architectural and kinetic interpretation model for breast MR images. *Acad Radiol* 2001;8(7):591-7.
- [6] Liberman L, Morris EA, Lee MJ, et al. Breast lesions detected on MR imaging: features and positive predictive value. *AJR* 2002;179(1):171-8.